JACS
JOURNAL OF THE AMERICAN CHEMICAL SOCIETY

Article

Extremely fast hydrogen atom transfer between nitroxides and HOO• radicals and implication in catalytic co-antioxidant systems

Andrea Baschieri, Luca Valgimigli, Simone Gabbanini, Gino DiLabio, Eduardo Romero-Montalvo, and Riccardo Amorati

J. Am. Chem. Soc., **Just Accepted Manuscript** • DOI: 10.1021/jacs.8b06336 • Publication Date (Web): 19 Jul 2018

Just Accepted

ACS Publications

is published by the American Chemical Society. 1155 Sixteenth Street N.W., Washington, DC 20036

Extremely fast hydrogen atom transfer between nitroxides and HOO• radicals and implication in catalytic co-antioxidant systems

Andrea Baschieri,[a] Luca Valgimigli,*[a] Simone Gabbanini,[b] Gino DiLabio,[c,d] Eduardo Romero-Montalvo,[c] Riccardo Amorati*[a]

[a] Department of Chemistry "G. Ciamician", University of Bologna, Via S. Giacomo 11, 40126 Bologna, Italy. E-mail: riiccardo.amorati@unibo.it; luca.valgimigli@unibo.it

[b] R&D division, BeC s.r.l. Via C. Monteverdi 49, 47122 Forlì, Italy

[c] Department of Chemistry, University of British Columbia, 3247 University Way, Kelowna, British Columbia, Canada

[d] Faculty of Management, University of British Columbia, 1137 Alumni Ave, Kelowna, British Columbia, Canada

Abstract: We report a novel co-antioxidant system based on TEMPO (2,2,6,6-tetramethylpiperidine-1-oxyl) that, in biologically-relevant model systems, rapidly converts chain-carrying alkylperoxyl radicals to HOO•. Extremely efficient quenching of HOO• by TEMPO blocks the oxidative chain. Rate constants in chlorobenzene were measured to be 1.1×10^{9} $M^{-1}s^{-1}$ for the reductive reaction TEMPO + HOO• → TEMPOH + O_2 and 5.0×10^{7} $M^{-1}s^{-1}$ for the oxidative reaction TEMPOH + HOO• → TEMPO + H_2O_2. These rate constants are significantly higher than that associated with the reaction of HOO• with α-tocopherol, Nature's best lipid soluble antioxidant ($k = 1.6\times10^{6}$ $M^{-1}s^{-1}$). These data show that in the presence of ROO•-to-HOO• chain-transfer agents, which are common in lipophilic environments, TEMPO/TEMPOH couple protects organic molecules from oxidation by establishing an efficient reductive catalytic cycle. This catalytic cycle provides a new understanding of the efficacy of the antioxidant capability of TEMPO in non-aqueous systems and its potential to act as a chemoprotective against radical damage.

Introduction

Nitroxides are stable and persistent free radicals that find wide use in (bio)chemical applications, such as polymerization catalysts, spin labels, organic battery electrodes, and antioxidants.[1-5] In biomedical applications, recent work explored the use of nitroxides as antioxidants in the inhibition of ferroptosis,[6,7] protection from retinopathy,[8] and from ischemia-reperfusion.[9] Nitroxides are also crucial intermediates formed during the antioxidant action of aromatic amines and of hindered amine light stabilizers (HALS), which are widely used as polymer and oil stabilizers,[10] and as active moieties of nanoantioxidants.[11] In these examples, nitroxides protect organic molecules from autoxidation.

Lipid peroxidation is sustained by alkylperoxyl radicals (ROO•), which are formed from the reaction of carbon-centered radicals (R•) with O_2 that is ubiquitous in biologically relevant environments.[12] In water, nitroxides react very quickly with alkylperoxyl radicals (k = 2.8–10 × 10^6 $M^{-1}s^{-1}$) leading to the oxidation of the nitroxide to form the oxoammonium cation (Reaction 1), via proton-coupled electron transfer mechanisms.[3,5] The formation of oxoammonium ion is also the key step in the reaction with superoxide (HOO• / $O_2^{\bullet-}$) in water, where nitroxides behave in a catalytic fashion by cycling between the oxoammonium and the nitroxide redox states (Reactions 2 and 3).[4]

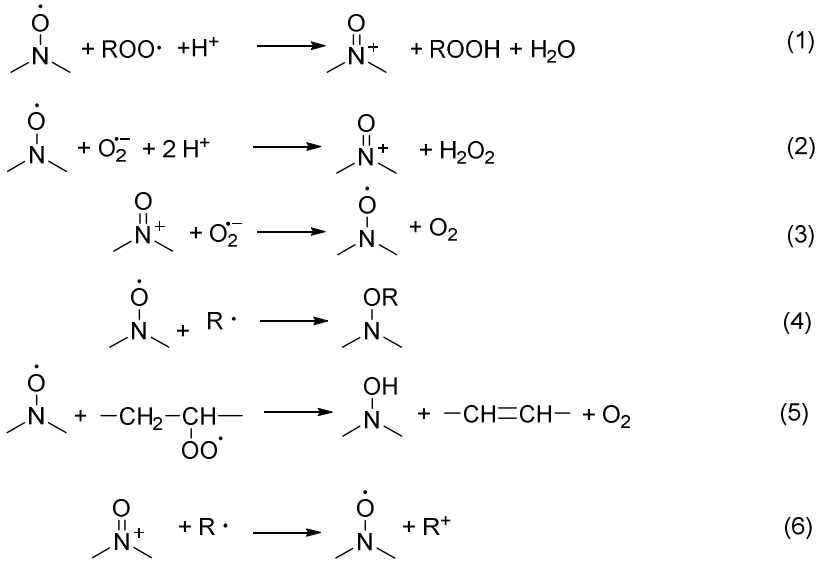

These reactions explain the antioxidant activity of nitroxides in aqueous systems.[13] However, this mechanism cannot be invoked in the many cases in which nitroxides reduce the extent of autoxidation in lipophilic environments such as the interior of membranes[8,14] and in oils,[11] particularly near room temperature. In fact, dialkyl nitroxides are only weak retardants of the autoxidation of hydrocarbons and of polyunsaturated lipids in model apolar solvents.[15] The limited activity of nitroxides in this

connection is due to the quenching of alkyl radicals (Reaction 4)[15] or to the (inefficient) H-atom transfer reaction from a C-H bond of the alkyl peroxyl radical to the nitroxide to afford the corresponding hydroxylamine (Reaction 5).[16] Some of us reported the first case of efficient quenching of ROO• by nitroxides in non-aqueous solvents wherein the reaction of dialkyl nitroxides with ROO• in MeCN can be substantially accelerated by the addition of a weak acid.[17] The proposed mechanism is a proton-coupled electron transfer from the nitroxide and the acid to ROO•, producing the corresponding hydroperoxide and the oxoammonium salt (Reactions 1 and 6, where H^+ is provided by a carboxylic acid). [10,17]

Interestingly, nitroxides have been reported to act as catalytic antioxidants in organic solvents when the chain-carrying radicals are hydroperoxyl (HOO•), such as during the autoxidation of alcohols and amines at temperatures of 323-348K. Inhibition was suggested to occur via reactions 7 and 8, where 7 is the rate determining step.[18b]

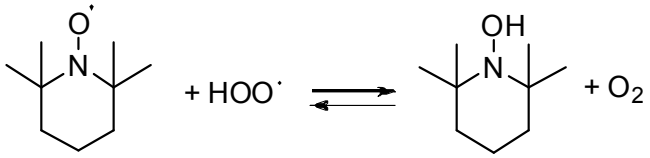

(7)

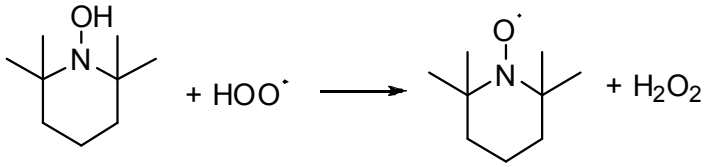

(8)

Pliss et al. recently reported that 2,2,6,6-tetramethylpiperidine-1-oxyl (TEMPO) catalytically inhibited the autoxidations of substituted ethylenes and 1,3-butadienes at 323 K, in which reactions HOO• serves as the chain carrying radical.[19]

Based on these observations, we envisaged that the catalytic quenching of HOO• could be the key to a general strategy to achieve efficient inhibition of autoxidation in non-aqueous systems. Although reaction 7 could explain the observed antioxidant behavior, it has not been demonstrated directly.[20] With the aim of rationally exploiting the catalytic antioxidant activity of nitroxides, we report herein the first experimental measurement of the rate constants and the kinetic solvent effect of reactions 7 and 8, in the case of prototypical nitroxide TEMPO and of its hydroxylamine TEMPOH. We also describe how co-antioxidants present in common lipophilic biomaterials interact with TEMPO to

remove chain-carrying alkylperoxyl radicals through a highly efficient catalytic cycle. We further discuss how this catalytic system can be used to underpin the design novel co-antioxidant systems.

Results and discussion

1) Experimental determination of the values of k_7 and k_8

Hydroperoxyl (HOO•) is involved in the initiation of lipid peroxidation of membranes when exposed to a source of superoxide,[21] as well in the propagation of the peroxidative chain of alkylamines,[22] alcohols,[18b] and cyclohexadiene derivatives[23] in non-aqueous media. To study this reaction, we measured the rate of the autoxidation of 1,4-cyclohexadiene (CHD), initiated at constant rate by azobisisobutyronitrile (AIBN) at 30 °C, by measuring the O_2 uptake as previously reported (see Scheme 1).[23,24]

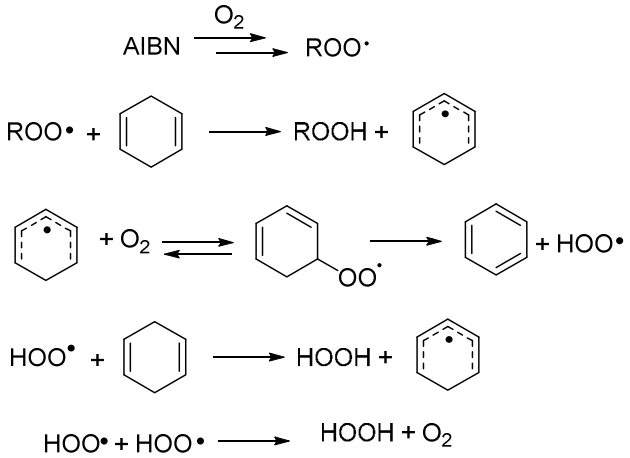

Scheme 1. Autoxidation mechanism of 1,4-cyclohexadiene (CHD).

The rate of the CHD autoxidation was monitored by O_2 consumption; Figure 1A shows that this autoxidation was strongly inhibited by the addition of TEMPO. Preliminary experiments showed that the direct reaction between TEMPO and CHD (i.e. without the radical initiator AIBN) does not occur on the time-scale of the autoxidation experiments, see Figure 1S.

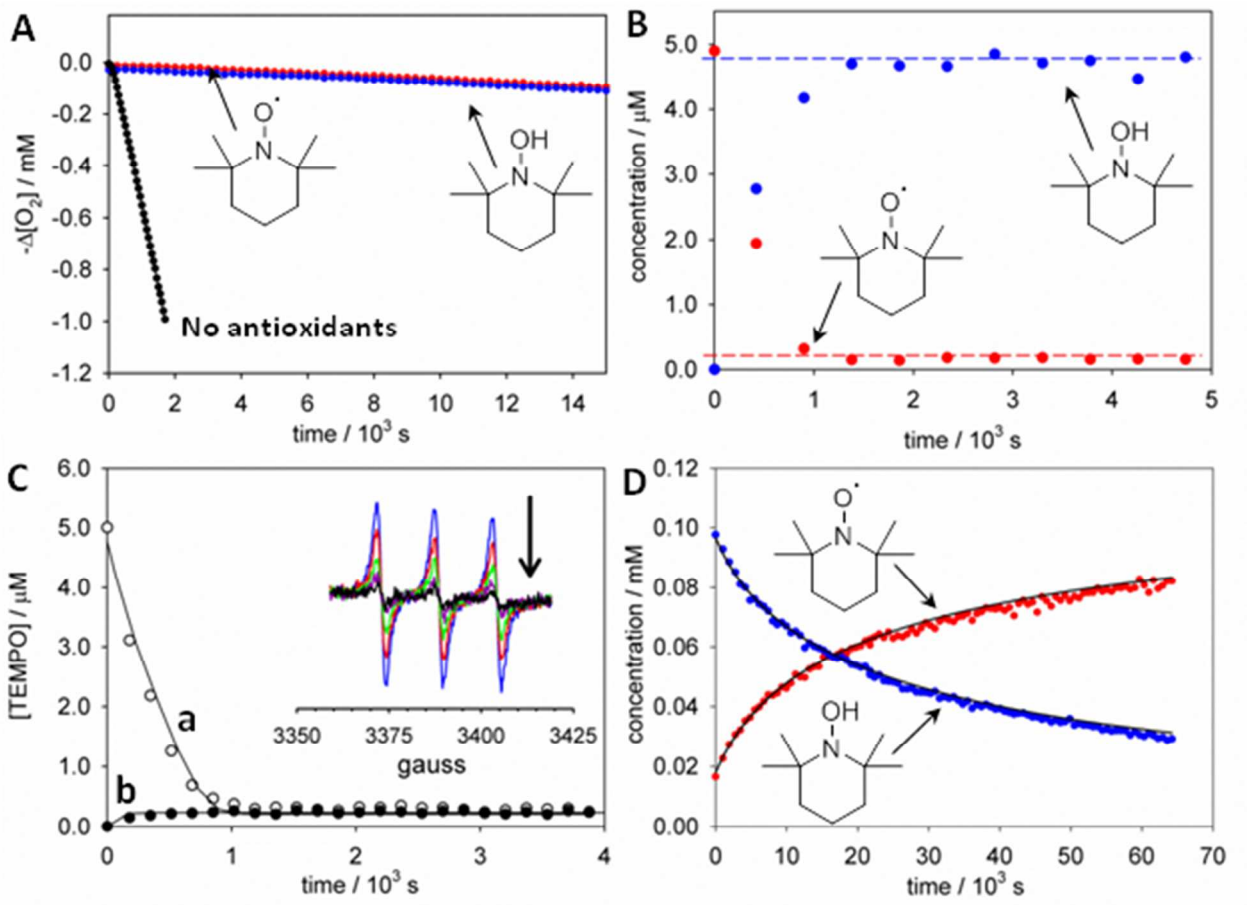

Figure 1. A) Inhibition of the O_2 consumption during the autoxidation of CHD in PhCl initiated by AIBN at 30° in the presence of either 5 μM of TEMPO (red line) or 5 μM of TEMPOH (blue line) and simulation with COPASI (solid lines). B) Concentrations of TEMPO and TEMPOH under the same conditions as panel A. C) EPR spectroscopic (dots) determination and simulation with COPASI (solid lines) of the concentration of TEMPO during CHD autoxidation in the presence of (a) TEMPO (inset: EPR spectra) or (b) TEMPOH, both at 5 μM. D) Time evolution of the concentration of TEMPO and TEMPO monitored by GC-MS on exposing a solution of TEMPO to atmospheric oxygen at 303 K.

On the other hand, during the autoxidation there is a rapid quantitative reduction of TEMPO to TEMPOH as demonstrated through GC-MS (Figure 1B, Figure 2S and Figure 3S), UPLC-MS (Figure 4S) analysis of the reaction mixture. These data demonstrate the reduction of TEMPO to TEMPOH whilst showing no formation of the (most expected) oxidized oxoammonium species. Parallel autoxidation experiments monitored by EPR spectroscopy (Figure 1C and Figure 5S) showed a time-

evolution of TEMPO that was superimposable on the CG-MS data, and these were used for quantitative analysis of reaction kinetics (*vide infra*).

The conversion of TEMPO to TEMPOH is incomplete. After the first few minutes of autoxidation, a steady-state is reached wherein the [TEMPO] and [TEMPOH] are in a ratio of ~96:4, and this ratio was maintained throughout the experiment (Figure 1B). This suggests that TEMPOH is oxidized back to TEMPO through the reaction with chain-carrying HOO• radicals (Reaction 8, as suggested by Denisov[18] and Pliss[19]) during the inhibition process. Indeed, when tested on the autoxidation of CHD, TEMPOH had an identical antioxidant effect to that of TEMPO (Figure 1A).

We investigated other potentially competing reactions that may lead to the oxidation of the hydroxylamine. TEMPOH is efficiently oxidized to TEMPO by atmospheric oxygen: This is a well-known reaction that challenges the purification of the hydroxylamine following its synthesis (Reaction -7).

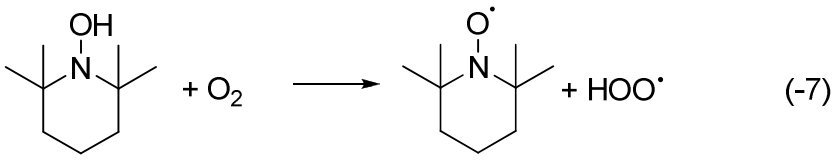

(-7)

Since this reaction would deplete the hydroxylamine and yield chain-carrying hydroperoxyl radicals, it would have pro-oxidant effect, rather than an antioxidant effect as shown in Figure 1A. The kinetics of -7 was investigated using GC-MS to follow the disappearance of TEMPOH in the presence of O_2 in different organic solvents. The reaction was slow, with a $t_{1/2}$ of about 3 hours, and quantitatively yielded TEMPO (see Figure 1D, Scheme 1S, Figures 6S and 7S). Second order rate constants, k_{-7}, were measured to be 0.026 $M^{-1}s^{-1}$ and 0.016 $M^{-1}s^{-1}$ in PhCl and EtOAc, respectively, at 303 K (*vide infra*): The values that are too low to justify the steady states of TEMPO and TEMPOH, which require rapid interconversion.

In the polar aprotic solvents MeCN and AcOEt, the antioxidant abilities of TEMPO and TEMPOH were smaller than those measured in PhCl (O_2 consumption plots are shown Figure 8S and Figure 9S), suggesting that reactions 7 and 8 are negatively affected by hydrogen bonding with the solvent. This is expected for the transfer of a hydrogen atom linked to an electronegative atom.[25]

Autoxidation of CHD inhibited by TEMPO or TEMPOH in acetonitrile containing D_2O showed a dramatically smaller antioxidant effect with respect to the corresponding experiment in the presence of

H_2O (Figure 2 and Figure 10S). This deuterium kinetic solvent effect confirms that the key mechanism is the formal transfer of an H atom.

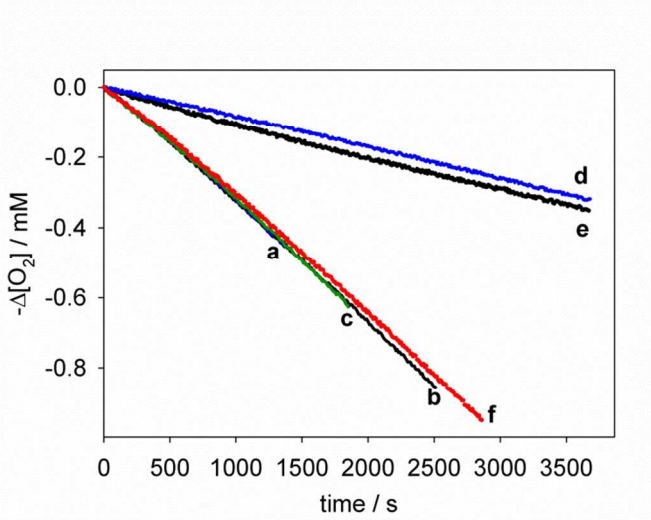

Figure 2. Autoxidation of CHD in MeCN without inhibitors (a) or in the presence of 1.3% v/v H_2O (b), 1.3% v/v D_2O (c), TEMPO (d), 1.3% v/v H_2O + TEMPO (e), 1.3% v/v D_2O + TEMPO (f).

The foregoing findings indicate that the reaction between TEMPO and HOO• (Reaction 7) can be explained as an efficient H-atom transfer to afford TEMPOH and O_2. A second important aspect of the results shown in Figure 1A is that the number of radicals trapped by each TEMPO molecule significantly exceeds the value of 1 that would be expected from a stoichiometric reaction between TEMPO and HOO•. As anticipated, this is explained by the fact that TEMPOH is also able to efficiently react with HOO•, with the formation of H_2O_2 and TEMPO (Reaction 8). Therefore, reactions 7 and 8 couple to produce a reductive catalytic cycle for TEMPO + HOO•. Notably, this cycle operates in a fashion that is alternative to the oxidative cycle previously established for TEMPO in aqueous solutions.

To obtain the values of rate constants k_7, k_{-7} and k_8, we quantitated by EPR spectroscopy the time-evolution of TEMPO during autoxidation experiments inhibited either by TEMPO or TEMPOH. The findings from these measurements matched our chromatographic results. Therefore, TEMPOH/TEMPO relative concentrations determined by EPR and CG-MS served as constraints for the analysis of the O_2 consumption traces of CHD autoxidations performed using the kinetic simulation software "COPASI".[26] The numerical analysis of O_2 consumption plots required literature values of the rate constants for CHD autoxidation,[23] and the rate of initiation that was measured in our preliminary

experiments using the inhibition period method (see Scheme 2S, Table 1S and Figure 11S).[27] The procedure resulted in excellent fits of the experimental traces and yielded values of k_7 and k_8 in PhCl and AcOEt, which are reported in Table 1. A similar analysis of the kinetics of TEMPOH disappearance under O_2 (Figure 1D) provided the values of k_{-7} (Table 1).

Table 1. Values of k_7, k_{-7} and k_8 ($M^{-1}s^{-1}$). The ratio of the rate constants reflects the effect of solvent on the reactions.

rate constant	PhCl[a]	AcOEt[a]	solvent effect
k_7	$(1.1\pm0.1) \times 10^9$	$(1.9\pm0.3) \times 10^7$	58
k_{-7}	$(2.6\pm0.2) \times 10^{-2}$	$(1.6\pm0.1) \times 10^{-2}$	1.6
k_8	$(5.0\pm0.4) \times 10^7$	$(1.7\pm0.2) \times 10^6$	29

[a] mean of three measures, ±Standard Deviation.

The values reported in Table 1 indicate that the reaction between TEMPO and HOO• in PhCl occurs with nearly diffusion-controlled rate constant, in alignment with the large exothermicity of the reaction, ($\Delta H \approx -9$ kcal/mol in DMSO).[28] The results also indicate that reaction 8 is one order of magnitude slower than reaction 7, making it the rate-determining step of the catalytic antioxidant cycle.

In a polar solvent, k_7 decreases by 58-fold. The kinetic solvent effect (KSE) in k_7 can be attributed to the hydrogen bonding between HOO• and the solvent (i.e. S···HOO•), which renders it less reactive as an H-atom donor (see Scheme 2A). Unexpectedly, k_8 in PhCl is significantly larger than the rate constant for the reaction between TEMPOH and ROO• ($k = 1.6 \times 10^6$ $M^{-1}s^{-1}$ at 303 K in the case of the peroxyl radicals derived from styrene).[17] This result can be explained by considering the smaller steric requirement of HOO• relative to ROO•. The value of k_8 decreases in AcOEt relative to the rate constant in PhCl by an amount that is about half of the decrease observed for k_7. The decrease in k_8 likely result from two parallel effects: The formation of a weak TEMPOH···S hydrogen bond complex,[17] and the "remote" H-bond effect in the abstracting radical, wherein S···HOO• has a somewhat lower reactivity than HOO• toward H-atom abstraction (Scheme 2B).[24a] The negligible KSE found for k_{-7} can be attributed to a weak H-bond of TEMPOH with solvents, in-line with previous findings. For

comparison, the KSE for the reaction of TEMPOH with alkylperoxyl radicals was $k_{inh}^{PhCl} / k_{inh}^{MeCN} = 1.3$ at 303 K.[17]

From the measured values of k_7 and k_{-7}, the free energy change of the TEMPO + HOO• reaction is determined to be -14.5 kcal/mol and -12.4 kcal/mol in PhCl and AcOEt, respectively.

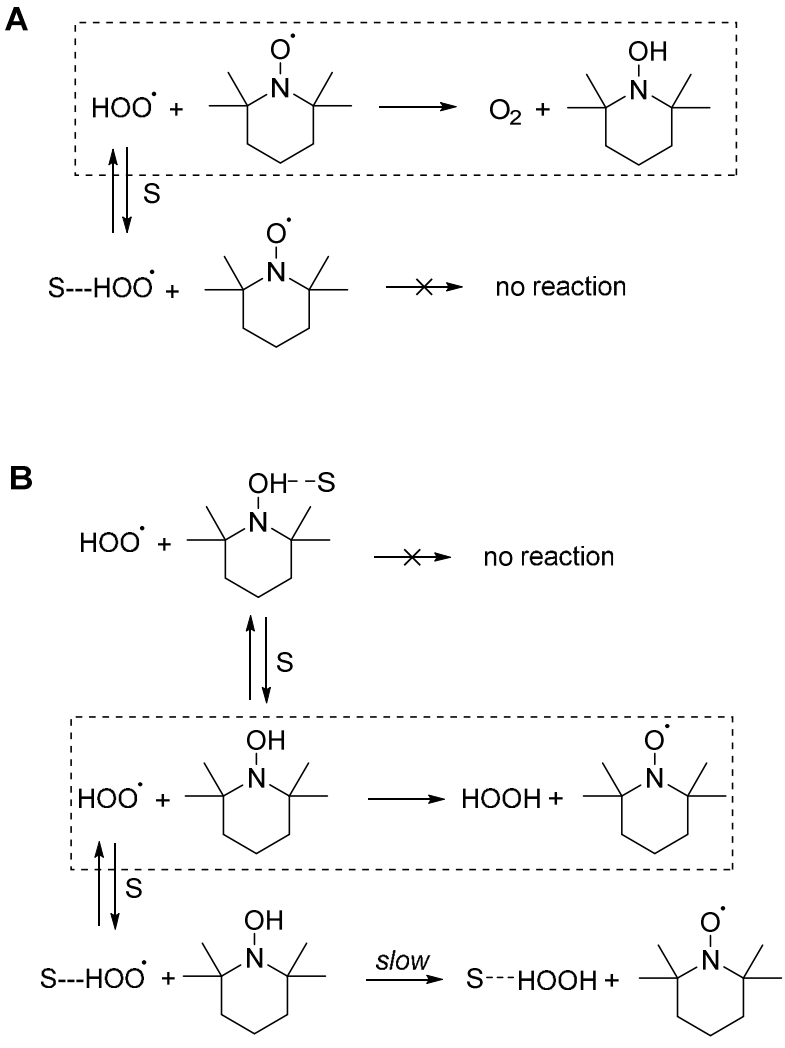

Scheme 2. Kinetic solvent effect on the reactions of HOO• with TEMPO (A) and TEMPOH (B).

The possibility that singlet O_2 is formed in Reaction 7 was considered, but it was discounted on the basis of results from autoxidation experiments in the presence of the $^1O_2$ trap 9,10-diphenylanthracene,

as the typical UV-vis spectrum of the trap was unchanged throughout the reaction (see Figure 12S).[29] The results of theoretical calculations, (see below) also discount the formation of $^1O_2$ in reaction 7.

2) Theoretical calculation of the barriers of reactions 7 and 8

We began our modeling efforts with an exploration of the spin state associated with reaction 7. We considered the possibility that the reaction might occur on the singlet spin surface, thereby generating $^1O_2$. Transition state (TS) structures for the hydrogen atom transfer reaction involving the triplet and open-shell singlet systems were examined, and both were found to be genuine TSs with single imaginary vibrations along the hydrogen atom transfer coordinate. At the level of theory employed in the examination of reactions 7 and 8 more generally (see below), i.e. CAM-B3LYP-D3/aug-cc-pVTZ//B3LYP-D3/6-31+G(d,p),[30] the triplet TS was found to be 2.4 kcal/mol lower in electronic energy than the singlet. Additional calculations were performed in order to assess the sensitivity of the triplet-singlet TS energy difference to the level of theory. Single-point energy calculations using the B2PLYPD3[31] and DSDPBEP86[32] double-hybrids and the wavefunction-based composite CBS-QB3[33] method verified that the triplet TS was lower than the singlet by 3.2, 2.6 and 2.3 kcal/mol, respectively. Thermal and entropic corrections to fee energy further increase the triplet-singlet separation by about 0.8 kcal/mol. On the basis of these results, we conclude that reaction 7 occurs on the triplet surface with a rate constant that is at least two orders of magnitude higher than that associated with the singlet surface. The results of our calculations and our $^1O_2$ trap experiments support the conclusion that the reaction occurs on the triplet spin surface.

The calculated relative free energies associated with reaction 7 on the triplet surface are summarized in Figure 3a. In PhCl, the reactants form a hydrogen-bonded pre-reaction complex (ΔG_{298} = -1.0 kcal/mol) prior to surmounting a relative free energy barrier of 5.7 kcal/mol. The computed transition state (TS) structure is shown in Figure 4a. The reaction is calculated as overall exergonic by -10.4 kcal/mol and leads to the formation of TEMPOH and $^3O_2$. Calculations using AcOEt as the solvent give a barrier of 6.3 kcal/mol, which is in qualitative agreement with our experimental findings. These results are consistent with the stronger hydrogen-bond accepting ability of AcOEt compared to PhCl, and the consequences this has on the reaction rate constants.[34]

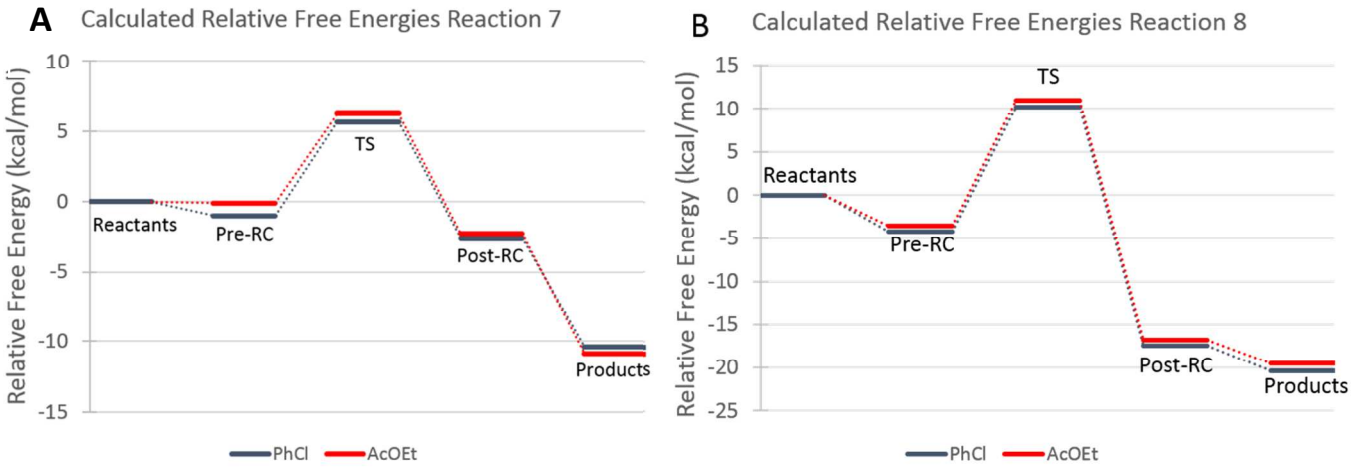

Figure 3. Calculated free energy reaction coordinate associated with reactions A) **7** and B) **8**, relative to reactants. Key: Pre-RC = pre-reaction complex, TS = transition state complex, Post-RC = post-reaction complex.

Figure 3b shows the calculated results for reaction 8. The results demonstrate that a very strong hydrogen-bonded, pre-reaction complex forms between TEMPOH and HOO•, viz. ΔG = -4.2 kcal/mol in PhCl, see Fig. 4b. This double hydrogen bond results from a strong orbital interaction between the TEMPOH nitrogen lone-pair and the O-H σ* orbital of HOO• and a weaker interaction between a HOO• O lone-pair and the O-H σ* orbital of TEMPOH. The zero-point corrected electronic energy calculated for this hydrogen bond is 16.4 kcal/mol in the gas-phase. For comparison, the high-level ab initio value for the strong hydrogen bonding in the uracil-uracil dimer is 17.4 kcal/mol.[35] Relative to reactants, the free energy barrier to hydrogen atom transfer is computed to be 9.1 kcal/mol (TS shown in Figure 4c) and is strongly downhill to products. In AcOEt, calculations predict weaker hydrogen bonding and a higher reaction barrier, consistent with the experimental results.

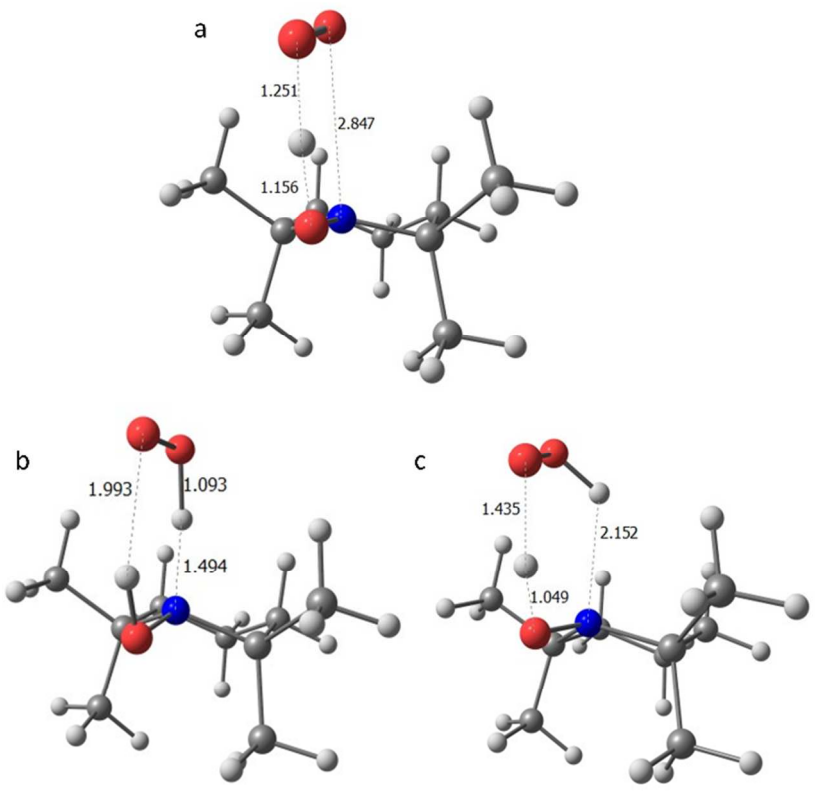

Figure 4. Computed structure of the a) TS associated with reaction 7, and the b) pre-reaction and c) TS associated with reaction 8. N = blue; O = red; C = grey; H = white. Distances are in Angstroms.

The computed TS structures associated with reactions 7 and 8 are shown in Figure 4 (a,c), along with the strongly hydrogen-bonded pre-reaction for reaction 8 (Fig. 4b). We note that the TS show in Fig. 4a has a cisoid structure. This is expected on the basis of previous work that showed that hydrogen atom transfer reactions in which lone pair-lone pair overlap can occur in the TS develop partial bonding character that stabilize the structures relative to transoid TSs wherein such overlap cannot occur (see Figure 13S).[36]

3) Catalytic co-antioxidant systems

Our results show that TEMPO is a powerful catalytic quencher of HOO• in non-aqueous solvents. However, it is not obvious how this property is connected to antioxidant activity toward substrates that autoxidize through ROO• formation, such as the unsaturated lipids in bio-membranes. We

hypothesized that TEMPO unleashes its antioxidant activity in the presence of molecules that act as co-antioxidants able to transfer the chain-reaction from ROO• to HOO•. Indeed, a number of structures commonly found in natural oxidizable materials or in biological systems could serve as chain-transfer co-antioxidants. For instance, CHD is the model for widespread terpenoid components of vegetable oils (e.g. α-terpinene, γ-terpinene, α-phellandrene, etc.) known to oxidize via HOO•.[37] 1,4-Hydroquinones are ubiquitous in biological systems (*e.g.* ubiquinol) and are known to form HOO• upon reaction with ROO•.[38] Additionally, biologically ubiquitous aliphatic amines[22] and alcohols[18] are known to form HOO• during their autoxidation. Since k_7 and k_8 far exceed the rate constants of reactions of ROO• with common chain-breaking antioxidants, it is reasonable to expect that the TEMPO/TEMPOH system would be efficient even in the presence of relatively small amounts of co-antioxidants.

We demonstrate the efficacy of catalytic co-antioxidant system by studying the autoxidation of styrene, which is a typical substrate that forms ROO•. Inhibition of this autoxidation by TEMPO is sought in the presence of CHD and three other model compounds that yield HOO• upon reaction with free radicals, namely 2,5-di-*tert*-butylhydroquinone (QH_2),[38] trimethylamine[22] and benzylic alcohol[39] – as summarized in Scheme 3.

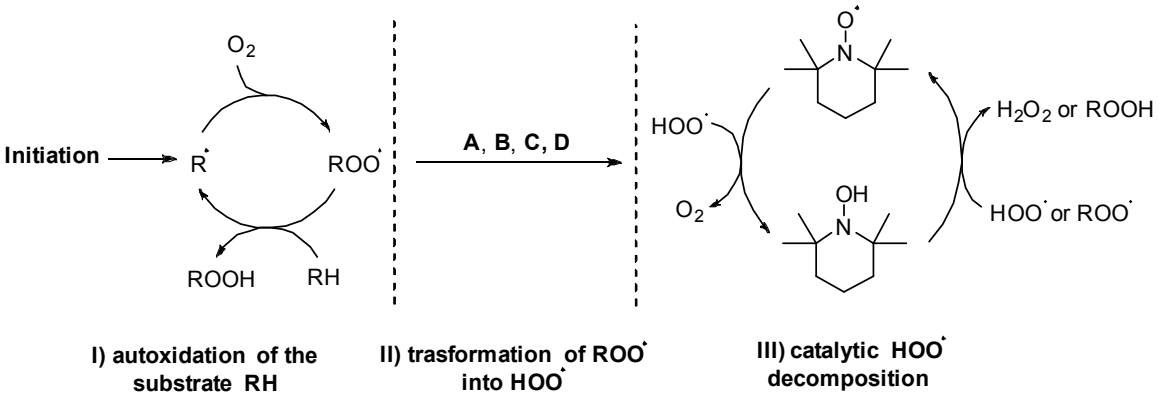

Scheme 3. Mechanism explaining the co-antioxidant effect of TEMPO in the presence of (A) 1,4-cyclohexadienes, (B) triethylamine, (C) 1,4-hydroquinones or (D) benzyl alcohol.

The results presented in Figure 5 provide support for our co-antioxidant hypothesis. Styrene autoxidation is inhibited nearly to the point of elimination by the CHD-TEMPO, (panel A), QH_2-

TEMPO (panel B), Et_3N-TEMPO (panel C) co-antioxidant couples. Significant, albeit incomplete, inhibition is obtained with the $PhCH_2OH$-TEMPO co-antioxidant couple (panel D).

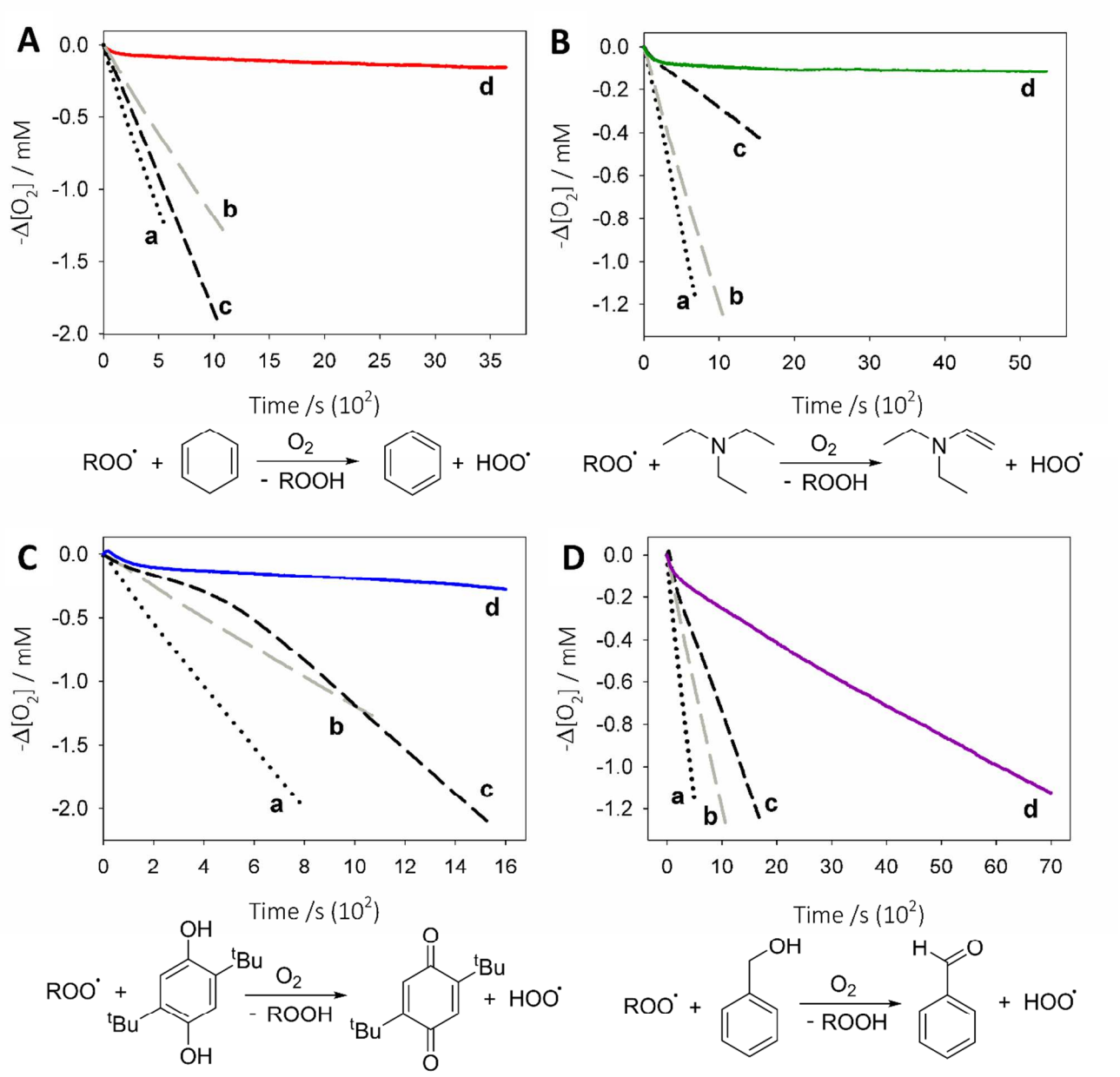

Figure 5. O_2 consumption during the autoxidation of styrene (4.3 M) in chlorobenzene initiated by AIBN at 30° without antioxidants (a in panels A, B, C and D), or in the presence of: TEMPO 5 μM (b in panels A, B, C and D), CHD 0.27 M or CHD 0.27 M and TEMPO 5 μM (c and d in panel A), Et_3N 0.018 M or Et_3N 0.018 M and TEMPO 5 μM (c and d in panel B), QH_2 5 μM or QH_2 5 μM and

TEMPO 5 μM (c and d in panel C), $PhCH_2OH$ 0.24 M or $PhCH_2OH$ 0.24 M and TEMPO 5 μM (c and d in panel D).

Inspection of the kinetic traces in Fig. 5 reveals that while some chain-transfer co-antioxidants like QH_2 and Et_3NH are able to retard autoxidation on their own due to quenching of ROO• radicals and replacing with faster terminating HOO•, addition of micromolar amounts of TEMPO boosts the antioxidant protection by largely suppressing the radical chain. This co-antioxidant system out-performs Nature's best antioxidant, α-tocopherol (see Figure 14S). More importantly, and unlike typical antioxidants that quench peroxyl radicals on stoichiometric basis by blocking one to two radicals per antioxidant molecule, TEMPO acts in a catalytic fashion by inhibiting autoxidation over a longer duration, the extent of which depends on the availability of the chain-transfer agent. The relatively lower performance of $PhCH_2OH$-TEMPO co-antioxidant couple can be explained by the lower efficiency of the alcohol in affording ROO• to HOO• chain-transfer. Despite the lower efficiency, we were able to obtain relevant co-oxidant activity with TEMPO even in the case of unactivated primary alcohol *n*-octanol (Figure 15S). In general, the very large rate constants for HOO• quenching by both TEMPO and TEMPOH (reactions 7 and 8) suggest that, under most common experimental conditions, the limiting step governing the efficacy of the co-antioxidant system lies in the chain-transfer process.

To provide proof-of-concept of the validity of our "co-antioxidant hypothesis" in a biological context, we investigated the oxidation of turpentine oil. Turpentine oil, obtained from pine wood, is a commodity produced on a scale of ca. 250,000 tons annually, and has a broad range of uses: from the manufacturing of paints and coatings, to that of plastics, food, cosmetics and pharmaceuticals.[40] It is based on α-pinene, that undergoes facile autoxidation mediated by alkylperoxyl radicals,[41] a process that may be involved in its toxicity.[42] This natural material also contains variable minor amounts of other components such as α- and γ-terpinene (*e.g.* 0.95% and 1.65%, respectively, in the specimen we investigated, see Figure 16S and Table 2S). Figure 6 shows that, at micromolar levels, TEMPO completely blocks turpentine autoxidation by exploiting the natural content of CHD-like terpinenes that act as co-antioxidant chain-transfer agents.[37b]

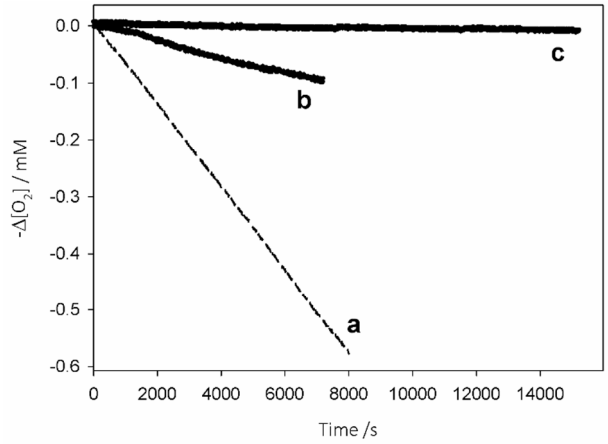

Figure 6. Oxygen consumption during the autoxidation of vegetable turpentine oil (*Pinus spp*) 75% V/V initiated by AIBN (0.05 M) in PhCl at 30°C in the absence of inhibitors (**a**) or in the presence of TEMPO 0.5 μM (**b**) or 5 μM (**c**).

Conclusions

The prototypical nitroxide TEMPO reacts very efficiently with HOO•, forming the corresponding hydroxylamine that is oxidized back to TEMPO by a second HOO•. The rate constants for these two processes are ca. 2.8 and 1.5 orders of magnitude faster, respectively, in comparison to Nature's most effective lipid-soluble, phenolic antioxidant α-tocopherol (k_{HOO} = 1.6×10^6 M^{-1}s^{-1} in PhCl at 30 °C).[24a] The efficiency of reactions 7 and 8 gives rise to a reductive catalytic cycle alternative to the established oxidative cycle observed in aqueous solution (Scheme 4). Our findings help resolve the long-standing mysterious antioxidant behavior of nitroxides in non-aqueous solvents, and open new insights in the role of nitroxides as HOO• sensors in the biological milieu.[43]

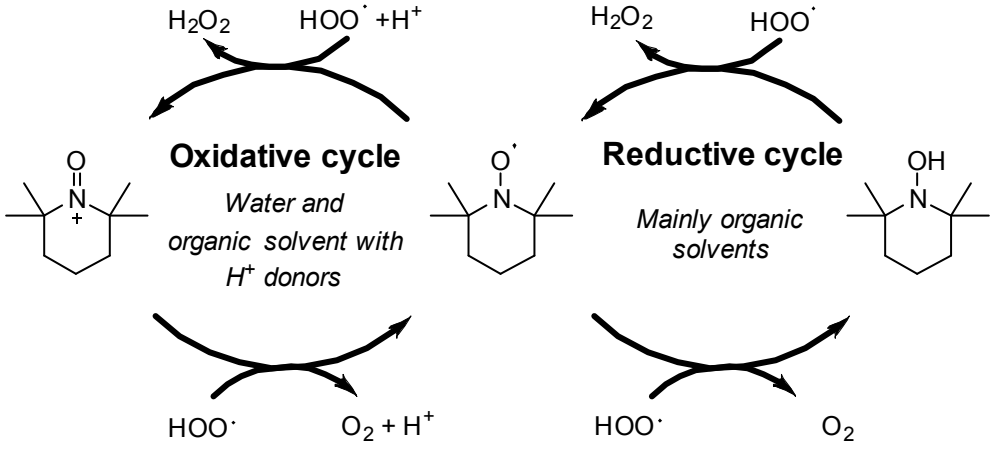

Scheme 4. Catalytic quenching of HOO• by TEMPO.

The catalytic antioxidant activity of TEMPO can be fully exploited in the presence of molecules able to transfer the chain-carrying radicals from ROO• to HOO•. Using cyclohexadienes, hydroquinones, alcohols and amines as model compounds in combination with TEMPO, we demonstrated the efficacy of these co-antioxidant systems in protecting naturally-occurring organic molecules from oxidation. The models are representatives of ubiquitous natural compounds in animal tissue, for example ubiquinol present in lipoproteins and in cellular membranes, and in plants (e.g. γ-terpinene[37]). Therefore, TEMPO can be used to provide extraordinary protection of biomaterials from the damage due to exposure to reactive oxygen species.

More generally, the effectiveness of the nitroxide-based catalytic cycle depends on the ability of the oxidizable substrate to form HOO• radicals during autoxidation,[44] and on the availability of suitable chain-transfer agents. We expect this chemistry to be very useful in the rational design of versatile, highly effective co-antioxidant systems.

Experimental section

Materials

All solvents (PhCl, MeCN, ethyl acetate) were of the highest grade commercially available (≥99,9% HPLC grade), and used as received. 1,4-cyclohexadiene (CHD, 97%) was percolated on alumina and silica before each experiment in order to remove traces of stabilizer. The initiator 2,2′-azobis(2-

methylpropionitrile) (AIBN), was recrystallized from methanol before use. 9,10-Diphenylanthracene (97 %), 2,2,6,6-tetramethylpiperidin-1-yl)oxyl, TEMPO (99 %), 2,2,5,7,8-pentamethyl-6-chromanol (97 %), 2,5-di-tert-butylhydroquinone (99%) and triethylamine (≥99%) were from Sigma Aldrich and were used as received. 1-Hydroxy-2,2,6,6-tetramethylpiperidine, TEMPOH, was synthesized by reducing TEMPO with sodium ascorbate as previously reported, and its characterization was consistent with literature values.[45] Turpentine was purchased from Muller & Koster and used as received. Its composition was determined by GC-MS, as reported in the Supporting Information.

Measurements of autoxidation rates

Autoxidation experiments were performed by measuring the oxygen consumption in a two-channel gas uptake apparatus, immersed in a thermostatted bath, based on Validyne DP15 pressure transducer.[24a,27,46] The rate of initiation (R_i) was calculated from preliminary set of experiments from the length of the inhibition period, t_{inh}, using 2,2,5,7,8-pentamethyl-6-chromanol (TOH) as a reference antioxidant during autoxidation of styrene.[47] The values of k_7 and k_8 (see manuscript) were obtained by numerical fitting of the O_2 consumption traces measured during the CHD autoxidation, by using the kinetic simulation software COPASI, freely available on the internet.[26] This method was previously used by our group and gave excellent results in the case of the CHD autoxidation inhibited by 2,2,5,7,8-pentamethyl-6-chromanol[24a] and in the case of non-classical antioxidants.[47] The reaction scheme used to simulate the experimental data is reported in Scheme 1S.

Determination of TEMPO and TEMPOH by GC-MS

The air equilibrated autoxidizing reaction mixture containing 10 % CHD in MeCN or PhCl or EtOAc with 0.05 M AIBN and TEMPO (5 μM) was sampled every 8 minutes and subjected to GC-MS analysis in a Trace 1310 – ISQ-QD GC-MS equipment (Thermo Fisher Scientific) equipped with a Combipal thermostatted autosampler (CTC) using a Zebron ZB-5 column 30m x 0.25 mm x 0.25 μm (Phenomenex) ramped from 50°C to 150°C at 20°C/min and eluted with He at 1.2 mL/min. Mass spectra were acquired in the range 40-650 amu and in multiple SIM mode at m/z 141, 142, 156, 157. Several calibration curves for TEMPO and TEMPOH were built with genuine standard solutions using either the full scan signal or the SIM at m/z 141 and 156 for TEMPO and at m/z 142 and 157 for the hydroxylamine ($R^2 > 0.99$) to confirm quantitative analysis under different acquisition modes.

Determination of TEMPO and TEMPOH by UPLC-MS

UPLC-MS analysis of the autoxidizing mixture in MeCN was performed with an Accela LCQ Fleet equipment (Thermo Fisher Scientific) on Hypersil Gold (Thermo) 100 mm x 2.1mm x 1.9 μm C18 column, thermostatted at 35°C, eluted with 1% aqueous formic acid (A) and acetonitrile (B) with gradient from 80%A-20%B to 30%A-70%B in 8 min, with flow of 250 μL/min. Injection volume was 2 μL. ESI+ spectra were recorded in the range m/z 50-500 with Ion spray voltage 5 KV, capillary voltage 15V and tube lens 110V. Since the signal-to-noise ratio for TEMPO was too low for reliable quantitative analysis, no calibration was performed, and analysis was used only to confirm GC-MS on qualitative grounds. Identification of TEMPO and TEMPOH and absence of $TEMPO^+$ was obtained by injecting genuine standards.

Determination of TEMPO by EPR spectroscopy

EPR experiments were performed with a Bruker Elexsys 500 spectrometer equipped with a Super X-Band ER049 microwave bridge and a quartz Dewar. Temperature was maintained at the desired value by a Bruker B-VT100 variable temperature unit and monitored before and after each experiment with a Delta OHM HD9218 type K thermocouple and was stable within ± 0.1°C.

An air saturated solution containing 10 % CHD in either PhCl or AcOEt with 0.05 M AIBN and TEMPO or TEMPOH (5 μM) was put in the cavity of the EPR spectrometer at 303K in an open quartz tube (4 mm ID). The time evolution of the concentration of TEMPO was monitored at regular intervals, both from the intensity of the first spectral line (a_N= 15.6 G, g = 2.0062) and from the double integral of the EPR spectrum.

Computational Details

The geometries of reactants, products, pre- and post-reaction complexes and the transition state structures were optimized using B3[48]LYP[49]-D3[50]/6-31+G(d,p) with the SMD[51] implicit solvent model. Frequency calculations at this same level of theory and basis set confirmed that the optimizations lead to local maxima for the transition state structures and local minima for all other species and provided thermal corrections to free energies. Single-point energies were calculated on all optimized structures using CAM-B3LYP[30]-D3/aug-cc-pVTZ basis sets with SMD solvent. All calculations were performed with the Gaussian-09 program.[52] Optimized geometries and calculated energies are reported in the ESI (Tables S2-S7).

Supporting Information

Additional experiments, experimental details, composition of turpentine, calculations and simulations (44 pages).

Acknowledgements

RA and LV thank the University of Bologna for funding. GAD thanks the National Sciences and Engineering Research Council, Canada Foundation for Innovation, and the BC Knowledge Development Fund for funding. ERM is grateful for the support provided by the Government of Mexico through CONACyT (Ph.D. Scholar/Scholarship 308773/472432).

References

1 a) Tesch, M.; Kudruk, S.; Letzel, M.; Studer, A. *Chem. Eur. J.* **2017**, *23* (25), 5915-5919; b) Hansen, K.-A.; Nerkar, J.; Thomas, K.; Bottle, S. E.; O'Mullane, A. P.; Talbot, P. C.; Blinco, J. P. *ACS Appl. Mater. Interfaces* **2018**, *10*, 7982−7988; c) Karthikeyan, G.; Bonucci, A.; Casano, G.; Gerbaud, G.; Abel, S.; Thomé, V.; Kodjabachian, L.; Magalon, A.; Guigliarelli, B.; Belle, V.; Ouari, O. Mileo, E. *Angew.Chem. Int. Ed.* **2018**, *57,*1366 –1370; d) Zhang, L.; Laborda, E.; Darwish, N.; Noble, B.B.; Tyrell, J. H.; Pluczyk, S.; Le Brun, A. P.; Wallace, G. G.; Gonzalez, J.; Coote, M. L.; Ciampi, S. *J. Am. Chem. Soc.* **2018**, *140*, 766−774; e) Prescott, C.; Bottle, S. E. *Cell Biochem. Biophys.* **2017**, *75*, 227–240.

2 a) Soule, B. P.; Hyodo, F.; Matsumoto, K.-I.; Simone, N. L.; Cook, J. A.; Krishna, M. C.; Mitchell, J. B. *Free Radic. Biol. Med.* **2007**, *42* (11), 1632–1650; b) Lewandowski, M.; Gwozdzinski, K. *Int. J. Mol. Sci*. **2017**, *18*, 2490.

3 Goldstein, S.; Samuni, A. *J. Phys. Chem. A* **2007**, *111* (6), 1066–1072.

4 Goldstein, S.; Merenyi, G.; Russo, A.; Samuni, A. *J. Am. Chem. Soc*. **2003**, 125 (3), 789–795.

5 Griesser, M.; Shah, R.; Van Kessel, A. T.; Zilka, O.; Haidasz, E. A.; Pratt, D. A. *J. Am. Chem. Soc.* **2018**, 140 (10), 3798–3808.

6 Krainz, T.; Gaschler, M. M.; Lim, C.; Sacher, J. R.; Stockwell, B. R.; Wipf, P. *ACS Cent. Sci.* **2016**, *2* (9), 653−659.

7 Zilka, O.; Shah, R.; Li, B.; Friedmann Angeli, J. P.; Griesser, M.; Conrad, M.; Pratt, D. A. *ACS Cent. Sci.* **2017**, 3 (3), 232−243.

8 Zareba, M.; Widomska, J.; Burke, J. M.; Subczynski, W. K. *Free Radic. Biol. Med*. **2016**, 101, 446–454.

9 Lahiani, A.; Hidmi, A.; Katzhendler, J.; Yavin, E.; Lazarovici, P. *ACS Chem. Neurosci*. **2016**, 7, 1452−1462.

10 Haidasz, E. A.; Meng, D.; Amorati, R.; Baschieri, A.; Ingold, K. U.; Valgimigli, L.; Pratt, D. A. *J. Am. Chem. Soc*. **2016**, *138* (16), 5290−5298.

11 a) Yoshitomi, T.; Hirayama, A.; Nagasaki, Y.; *Biomaterials* **2011**, *32*, 8021-8028; b) Valgimigli, L.; Baschieri, A.; Amorati, R. J. Mater. Chem. B **2018**, 6, 2036-2051.

12 Zielinski, Z. A. M.; Pratt, D. A. *J. Org. Chem*. **2017**, *82*, 2817−2825.

13 An exception to the oxidative cycle for the reaction with superoxide in water was reported by Samuni et al. in the case of the 2-ethyl-2,5,5-trimethyl-3-oxazolidinoxyl radical, which catalytically reacts with superoxide through the nitroxide-hydroxylamine couple. This reductive pathway, however, is less efficient than the oxidative one displayed by TEMPO. Samuni, A.; Krishna, C. M.; Riesz, P.; Finkelstein, E.; Russo, A. *J. Biol. Chem.* **1988**, *263*, 17921-17924.

14 Mobbili, G.; Crucianelli, E.; Barbon, A.; Marcaccio, M.; Pisani, M.; Dalzini, A.; Ussano, E.; Bortolus, M.; Stipa, P.; Astolfi, P. *RSC Adv*. **2015**, *5*, 98955–98966.

15 Pedulli, G. F.; Lucarini, M.; Pedrielli, P.; Sagrini, M.; Cipollone, M. *Res. Chem. Intermed*. **1996**, *22*, 1–14.

16 Tikhonov, I. V.; Pliss, E. M.; Bogoyavlenskii, D. A.; Berezin, M. P.; Sen, V. D. *Russ. Chem. Bull., Int. Ed.* **2015**, *64*, 2433—2437.

17 Amorati, R.; Pedulli, G. F.; Pratt, D. A.; Valgimigli, L. *Chem. Commun.* **2010**, *46*, 5139–5141.

18 a) Denisov, E. T. *Kinet. Catal*. **2015**, *56*, 56-70; b) Denisov, E. T. *Russ. Chem. Rev.* **1996**, *65*, 505-520.

19 Pliss, E. M.; Machtin, V. A.; Grobov, A. M.; Pliss, R. E.; Sirick, A. V. *Int. J. Chem. Kin*. **2017**, *49*, 173-181.

20 The rate constant for reaction 7 was estimated by Denisov as $\approx 10^8$ $M^{-1}s^{-1}$ (at 350 K) on the basis of thermodynamic considerations (ref. 18a) and was suggested to be rate-limiting compared to reaction 8 (ref. 18b).

21 Bedard, L.; Young, M. J.; Hall, D.; Paul, T.; Ingold, K. U. *J. Am. Chem. Soc.* **2001**, *123*, 12439–12448.

22 Howard, J. A.; Yamada, T. *J. Am. Chem. Soc.* **1981**, *103*, 7102−7106.

23 Howard, J. A.; Ingold, K. U. *Can. J. Chem.* **1965**, 43, 2729–2736.

24 a) Cedrowski, J.; Litwinienko, G.; Baschieri, A.; Amorati, R. *Chem. Eur. J.* **2016**, *22*, 16441 – 16445. b) Foti, M. C.; Sortino, S.; Ingold, K. U. *Chem. Eur. J.* **2005**, *11*, 1942 – 1948.

25 Litwinienko, G.; Ingold, K. U. *Acc. Chem. Res*. **2007**, *40*, 222-230.

26 Hoops, S.; Sahle, S.; Gauges, R.; Lee, C.; Pahle, J.; Simus, N.; Singhal, M.; Xu, L.; Mendes, P.; Kummer, U. *Bioinformatics* **2006**, *22*, 3067-3074.

27 Amorati, R.; Baschieri, A.; Morroni, G.; Gambino, R.; Valgimigli, L. *Chem. Eur. J.* **2016**, *22*, 7924 – 7934.

28 The bond dissociation enthalpies of TEMPOH is 72 kcal/mol, and that of H-OO• is 69 kcal/mol, in DMSO. Warren, J. J.; Tronic, T. A.; Mayer, J. M. *Chem. Rev*. **2010**, *110*, 6961–7001.

29 Tanaka, K.; Miura, T.; Umezawa, N.; Urano, Y.; Kikuchi, K.; Higuchi, T.; Nagano, T. *J. Am. Chem. Soc*. **2001**, *123*, 2530–2536.

30 Yanai, T.; Tew, D.; Handy, N. *Chem. Phys. Lett*. **2004**, *393*, 51-57.

31 Grimme, S. J. *Chem. Phys.* **2006**, *124*, 034108.

32 Kozuch, S.; Martin, J. M. L. *Phys. Chem. Chem. Phys*. **2011**, *13*, 20104–20107.

33 Montgomery Jr., J. A.; Frisch, M. J.; Ochterski, J. W.; Petersson, G. A. *J. Chem. Phys.* **2000**, *112*, 6532-6542.

34 Our modeling work does not reproduce the experimental relative free energies of reaction 7, or the correct ordering of the reaction exoergicities in the two solvents. This is a known shortcoming of implicit solvation methods when reproducing solvent effects due to specific H-bonding to the solvent. See: Guerra, M.; Amorati, R.; Pedulli, G. F. *J. Org. Chem.* **2004**, *69*, 5460-5467

35 DiLabio, G. A.; Johnson, E. R.; Otero-de-la-Roza, A. *Phys. Chem. Chem. Phys*. **2013**, *15*, 12821-12828.

36 a) DiLabio, G. A.; Johnson, E. R. *J. Am. Chem. Soc.* **2007**, *129*, 6199-6203; b) DiLabio, G. A.; Ingold, K. U. *J. Am. Chem. Soc.* **2005**, *127*, 6693-6699; c) Zielinski, Z.; Presseau, N.; Amorati, R.; Valgimigli, L.; Pratt, D. A. *J. Am. Chem. Soc.* **2014**, *136*, 1570−1578.

37 a) Foti, M. C.; Ingold, K. U. *J. Agric. Food Chem*. **2003**, *51*, 2758-2765; b) Amorati, R.; Foti, M. C.; Valgimigli, L. *J. Agric. Food Chem.* **2013**, *61*, 10835−10847.

38 Valgimigli, L.; Amorati, R.; Fumo, M. G.; DiLabio, G. A.; Pedulli, G. F.; Ingold, K. U.; Pratt, D. A. *J. Org. Chem*. **2008**, *73*, 1830-1841

39 Howard, J. A.; Korcek, S. *Can. J. Chem*. **1970**, *48*, 2165-2172.

40 https://ntp.niehs.nih.gov/ntp/htdocs/chem_background/exsumpdf/turpentine_508.pdf accessed on July 2018.

41 Neuenschwander, U.; Guignard, F.; Hermans, I. *ChemSusChem* **2010**, *3*, 75–84.

42 Amorati, R.; Foti, M.C. Oxidative stability and antioxidant properties of essential oils. In: Valgimigli, L. (Ed.), Essential oils as natural food additives, Nova Science Publishers, New York, **2012**. 75-95.

43 Chong, K. L.; Chalmers, B. A.; Cullen, J. K.; Kaur, A.; Kolanowski, J. L.; Morrow, B. J.; Fairfull-Smith, K. E.; Lavin, M. J.; Barnett, N. L.; New, E. J.; Murphy, M. P.; Bottle, S. E. *Free Radic. Biol. Med.* **2018**, https://doi.org/10.1016/j.freeradbiomed.2018.03.008

44 A very recent example appeared in the literature while this manuscript was in preparation is the production of HOO• in the autoxidation of alkenes at 70°C: Harrison, K. A.; Haidasz, E. A.; Griesser, M.; Pratt, D. A. *Chem. Sci.* **2018**, DOI: 10.1039/C8SC01575A.

45 Henry-Riyad, H.; Tidwell, T. T. *J. Phys. Org. Chem.* **2003**, *16*, 559-563.

46 Amorati, R.; Baschieri, A.; Valgimigli, L. *J. Chem*. **2017**, 6369358.

47 Amorati, R.; Lynett, P. T.; Valgimigli, L.; Pratt, D. A. *Chem. Eur. J.* **2012**, *18*, 6370 – 6379.

48 Becke, A. D. *J. Chem. Phys.* **1993**, *98*, 5648−5652.

49. Lee, C.; Yang, W.; Parr, R. G. *Phys. Rev. B* **1988**, *37*, 785−789.

50. a) Grimme, S.; Antony, J.; Ehrlich, S.; Krieg, H. *J. Chem. Phys.* **2010**, *132*, 154104. b) Grimme, S.; Ehrlich, S.; Goerigk, L. *J. Comput. Chem.* **2011**, *32*, 1456–1465.

51. Marenich, A. V.; Cramer, C. J.; Truhlar, D. G. *J. Phys. Chem. B* **2009**, *113*, 6378-6396.

52. Gaussian 09, Revision D.01, Frisch, M. J.; Trucks, G. W.; Schlegel, H. B.; Scuseria, G. E.; Robb, M. A.; Cheeseman, J. R.; Scalmani, G.; Barone, V.; Mennucci, B.; Petersson, G. A.; Nakatsuji, H.; Caricato, M.; Li, X.; Hratchian, H. P.; Izmaylov, A. F.; Bloino, J.; Zheng, G.; Sonnenberg, J. L.; Hada, M.; Ehara, M.; Toyota, K.; Fukuda, R.; Hasegawa, J.; Ishida, M.; Nakajima, T.; Honda, Y.; Kitao, O.; Nakai, H.; Vreven, T.; Montgomery, J. A., Jr.; Peralta, J. E.; Ogliaro, F.; Bearpark, M.; Heyd, J. J.; Brothers, E.; Kudin, K. N.; Staroverov, V. N.; Kobayashi, R.; Normand, J.; Raghavachari, K.; Rendell, A.; Burant, J. C.; Iyengar, S. S.; Tomasi, J.; Cossi, M.; Rega, N.; Millam, J. M.; Klene, M.; Knox, J. E.; Cross, J. B.; Bakken, V.; Adamo, C.; Jaramillo, J.; Gomperts, R.; Stratmann, R. E.; Yazyev, O.; Austin, A. J.; Cammi, R.; Pomelli, C.; Ochterski, J. W.; Martin, R. L.; Morokuma, K.; Zakrzewski, V. G.; Voth, G. A.; Salvador, P.; Dannenberg, J. J.; Dapprich, S.; Daniels, A. D.; Farkas, Ö.; Foresman, J. B.; Ortiz, J. V.; Cioslowski, J.; Fox, D. J. Gaussian, Inc., Wallingford CT, 2009.

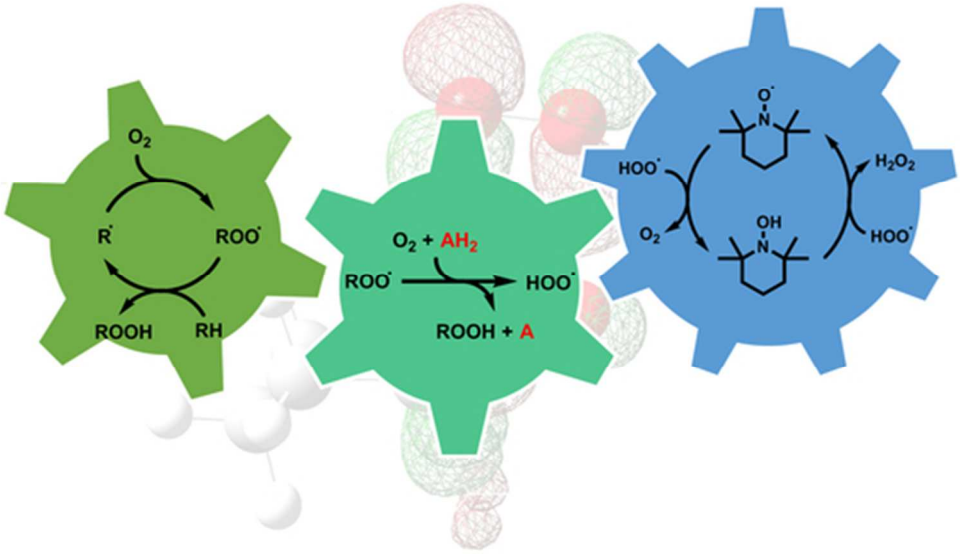

TOC

47x26mm (300 x 300 DPI)